Microscopic theory of quantum dot interactions with quantum light: Local field effect

G. Ya. Slepyan, A. Magyarov,* and S. A. Maksimenko
Institute for Nuclear Problems, Belarus State University, Bobruiskaya 11, 220050 Minsk, Belarus

A. Hoffmann
Institut für Festkörperphusik, Technische Universität Berlin, Hardenbergstrasse 36, 10623 Berlin, Germany
(Received 2 May 2007; published 27 November 2007)

A theory of both linear and nonlinear electromagnetic responses of a single quantum dot (QD) exposed to quantum light, accounting for depolarization induced local field has been developed. Based on the microscopic Hamiltonian accounting for the electron-hole exchange interaction, an effective two-body Hamiltonian has been derived and expressed in terms of the incident electric field, with a separate term describing the QD depolarization. The quantum equations of motion have been formulated and solved using the Hamiltonian for various types of the QD optical excitation, such as Fock qubit, coherent fields, vacuum state of electromagnetic field, and light with arbitrary photonic state distribution. For a QD exposed to coherent light, we predict the appearance of two oscillatory regimes in the Rabi effect separated by the bifurcation. In the first regime, the standard collapse-revival phenomenon does not reveal itself and the QD population inversion is found to be negative, while in the second one, the collapse-revival picture is found to be strongly distorted as compared to that predicted by the standard Jaynes-Cummings model. For the case of QD interaction with an arbitrary quantum light state in the linear regime, it has been shown that the local field induces a fine structure of the absorbtion spectrum. Instead of a single line with frequency corresponding to the exciton transition frequency, a duplet appears, with one component shifted by the amount of the local field coupling parameter. It has been demonstrated that the strong light–matter coupling regime arises in the weak-field limit. A physical interpretation of the predicted effects has been proposed.

DOI: 10.1103/PhysRevB.76.195328 PACS number(s): 73.21.−b, 78.67.Hc, 42.50.Ct

I. INTRODUCTION

The strong coupling regime between condensed matter and quantum light is a core issue of present day quantum optics. Realized by exposing the matter with intense quantum field, it can manifest itself in different quantum systems such as single atoms and ultracold atomic beams,[1] semiconductor heterostructures,[2,3] Bose-Einstein condensates,[4] etc. Albeit these systems are of different physical nature, their interaction with quantum light is governed by common rules. In the strong coupling regime, these systems enable +generation of different states of quantum light–single photons,[5] Fock states,[6] Fock qubits, and quantum states with an arbitrary photon number distribution.[7] These states constitute a basis for the quantum information processing[8,9] and quantum metrology.[10] In practice, the strong light–matter coupling regime can be realized in two ways: by combining the matter with a high-Q microcavity or by exposing the matter to an ultrashort intense pump pulse.

To describe strong coupling between an arbitrary two-level system and quantum light, the Jaynes-Cummings (JC) model is conventionally used.[11] One of the most fundamental phenomenon predicted within the JC model is the oscillation of the population between levels with the Rabi frequency (Rabi oscillations). However, the standard JC model does not account for a number of physical mechanisms, which, under certain conditions, may significantly influence the Rabi effect. The time-domain modulation of the field-matter coupling constant[7,12] and the interplay between classical driving field and quantized cavity field[7] can serve as examples. More advanced JC models involve additional interaction mechanisms and effects, such as dipole-dipole (d-d) interaction,[13,14] electron-phonon coupuling,[15,16] and self-induced transparency.[17] In particular, the d-d interaction between two quantum oscillators leads to their radiative coupling and, as a result, to an exchange by the excited state. That is, Rabi oscillations between these two oscillators occur; see Ref. 18 for a theory and Ref. 19 for the experimental observation in a double quantum dot (QD) system. As a whole, the observation and intensive study of excitonic Rabi oscillations[19–25] motivates the extension of the JC model to incorporate specific interactions inherent to a confined exciton in a host.

In this paper, we present a microscopic theory of the interaction of an isolated QD with quantum light for both weak and strong coupling regimes. We incorporate the local field correction into the JC model as an additional physical mechanism influencing the Rabi effect in a QD exposed to quantum light. In particular, the Rabi oscillations are shown to exist even in the limit of a weak incident field.

In the weak coupling regime, the local field effects in optical properties of QDs have been theoretically investigated in Refs. 26–34 for classical exposing light and in Ref. 35 for quantum light. In the latter case, it has been shown that for a QD interacting with Fock qubits, the local field induce a fine structure of the absorption (emission) spectrum: Instead of a single line with the frequency corresponding to the exciton transition, a doublet appears, with one component shifted to the blue (red). The intensities of components are completely determined by the quantum light statistics. In the limit of classical light and Fock states, the doublet is reduced to a singlet shifted in the former case and unshifted in the latter one.

The role of local fields in the excitonic Rabi oscillations in an isolated QD driven by classical excitation was investi-

gated in Ref. 36. Two different oscillatory regimes separated by the bifurcation have been predicted to exist. The Rabi oscillations were predicted to be nonisochronous and arising in the weak excitation regime. Both peculiarities have been experimentally observed by Mitsumori *et al.* in Ref. 25, where the Rabi oscillations of excitons localized to quantum islands in a single quantum well were investigated.

There exist several different physical interpretations of local field in QDs and, correspondingly, different ways of its theoretical description. The first model (scheme A in the terminology of Ref. 30) exploits the standard electrodynamical picture: By virtue of external field screening by charges induced on the QD surface (the quasistatic Coulomb electron-hole interactions), a depolarization field is formed, differentiating the local (acting) field in the QD and the external incident field. In this model, the total electromagnetic field is not pure transverse. Alternatively, only the transverse component is attributed to the electromagnetic field, while the longitudinal component is accounted for through the exchange electron-hole interactions (scheme B according to Ref. 30). Both approaches are physically equivalent and lead to identical results.

In the present paper, we build the analysis on the general microscopic quantum electrodynamical approach, where the local field correction originates from the exchange by virtual vacuum photons between electrons and holes forming the exciton and is thus a manifestation of the d-d interaction between electrons and holes (the dynamical Coulomb interaction).[13,14] The approach allows us to overcome a number of principal difficulties related to the field quantization in QDs.[37] In the analysis, an approximate solution of the many-body problem is built on the Hartree-Fock-Bogoliubov self-consistent field concept.[13] The self-consistent technique leads to a separate term in the effective Hamiltonian responsible for the interaction of operators and average values of physical quantities. Due to this term, the quantum-mechanical equations of motion become nonlinear and require a numerical integration.

The paper is arranged as follows. In Sec. II, we develop a theoretical model describing the QD–quantum light interaction. We formulate a model Hamiltonian with the separate term accounting for the local field correction and corresponding equations of motion. In Sec. III, we analyze the manifestation of local fields in the motion of the QD exciton in the absence of external field. In Sec. IV, we investigate the QD interaction with arbitrary states of quantum light in the weak driving field regime. Section V is devoted to the theoretical analysis of local field influence on the Rabi oscillations in the QD exposed to coherent states of light and Fock qubits. A discussion of the results obtained is presented in Sec. VI, and concluding remarks are given in Sec. VII.

II. QUANTUM DOT–QUANTUM LIGHT INTERACTION: THEORETICAL MODEL

A. Interaction Hamiltonian

In this section, we formulate the interaction Hamiltonian for a QD exposed to quantized field accounting for the local field correction. Later on, we exploit the Hamiltonian for the derivation of equations of motion, describing dynamical properties of this system.

As aforementioned, the local field in QD differs from the incident one due to the d-d electron-hole interaction. A general formalism, accounting for the d-d interactions in atomic many-body systems exposed to photons, has been developed in Refs. 13 and 14 and has been applied to nonlinear optics of Bose-Einstein condensates.[13,14] We extend this formalism to the case of the QD exciton driven by quantized light.

Consider an isolated QD exposed to quantized electromagnetic field. The electron-hole pairs in QD are assumed to be strongly confined; thus, we neglect the static Coulomb interaction between electrons and holes. We decompose the operator of the total electromagnetic field into two components. The first one, $\hat{\boldsymbol{\mathcal{E}}}_v$, represents a set of modes that do not contain real photons. The second component, $\hat{\boldsymbol{\mathcal{E}}}_0$, represents the set of modes emitted by the external source of light (real photons). Such a decomposition, as well as the subsequent separate consideration of the field components, is analogous to the Heisenberg-Langevin approach in the quantum theory of damping (see Ref. 1). The total Hamiltonian of the system "QD+electromagnetic field" is then represented as

$$\hat{\mathcal{H}} = \hat{\mathcal{H}}_0 + \hat{\mathcal{H}}_{\mathrm{ph}} + \hat{\mathcal{H}}_{\mathrm{vac}} + \hat{\mathcal{H}}_{I0} + \hat{\mathcal{H}}_{Iv}, \tag{1}$$

where $\hat{\mathcal{H}}_{0,\mathrm{ph},\mathrm{vac}}$ are the Hamiltonians of the QD free charge carriers, the incident photons and the virtual vacuum photons, respectively. The terms $\hat{\mathcal{H}}_{I0,Iv}$ describe the interaction of an electron-hole pair with incident quantum field $\hat{\boldsymbol{\mathcal{E}}}_0$ and with vacuum field $\hat{\boldsymbol{\mathcal{E}}}_v$, respectively. In the dipole approximation, these Hamiltonians are given by

$$\hat{\mathcal{H}}_{I0,Iv} = -\frac{1}{2}\int_V (\hat{\boldsymbol{\mathcal{P}}}\hat{\boldsymbol{\mathcal{E}}}_{0,v} + \hat{\boldsymbol{\mathcal{E}}}_{0,v}\hat{\boldsymbol{\mathcal{P}}})d^3\mathbf{r}, \tag{2}$$

where V is the QD volume and $\hat{\boldsymbol{\mathcal{P}}}(\mathbf{r},t)$ is the QD polarization operator. The Hamiltonian $\hat{\mathcal{H}}_{\mathrm{vac}}$ is as follows:

$$\hat{\mathcal{H}}_{\mathrm{vac}} = \sum_{k\lambda} \hbar\omega_k \hat{v}^\dagger_{k\lambda}\hat{v}_{k\lambda}, \tag{3}$$

where $\hat{v}^\dagger_{k\lambda}$ and $\hat{v}_{k\lambda}$ are the creation and annihilation operators of vacuum photons, k is the mode index, indices $\lambda = 1,2$ denote the field polarization. The operator of vacuum electromagnetic field $\hat{\boldsymbol{\mathcal{E}}}_v$ is determined as

$$\hat{\boldsymbol{\mathcal{E}}}_v = i\sum_{k\lambda} \sqrt{\frac{2\pi\hbar\omega_k}{\Omega}}\mathbf{e}_{k\lambda}(\hat{v}_{k\lambda}e^{i\mathbf{kr}} - \hat{v}^\dagger_{k\lambda}e^{-i\mathbf{kr}}), \tag{4}$$

where Ω is the normalization volume and $\mathbf{e}_{k\lambda}$ is the polarization unit vector.

As a first step in the development of our theory, we exclude from the consideration the vacuum photon operators $\hat{v}_{k\lambda}$ and $\hat{v}^\dagger_{k\lambda}$. For that purpose, we express them (and corresponding Hamiltonians $\hat{\mathcal{H}}_{\mathrm{vac}}$ and $\hat{\mathcal{H}}_{Iv}$) in terms of the polarization operator $\hat{\boldsymbol{\mathcal{P}}}$. Recalling the Heisenberg equation $i\hbar\partial\hat{v}_{k\lambda}/\partial t = -[\hat{\mathcal{H}}, \hat{v}_{k\lambda}]$, the expression as follows can be obtained:

$$\frac{\partial \hat{v}_{k\lambda}}{\partial t} = -i\omega_k \hat{v}_{k\lambda} + \hat{F}_{k\lambda}(t), \tag{5}$$

where $\hat{F}_{k\lambda}(t) = \sqrt{2\pi\omega_k/\hbar\Omega}\int_V \hat{\mathcal{P}}(\mathbf{r}',t)\mathbf{e}_{k\lambda}e^{i\mathbf{kr}}d^3\mathbf{r}'$. The solution of Eq. (5) is given by

$$\hat{v}_{k\lambda}(t) = \hat{v}_{k\lambda}(-\infty)e^{-i\omega_k t} + \int_{-\infty}^{t} \hat{F}_{k\lambda}(\tau)e^{-i\omega_k(t-\tau)}d\tau, \tag{6}$$

with the first term describing the free evolution of the reservoir modes (quantum noise) and the second one responsible for the exchange interactions. Further, we neglect the first term in Eq. (6), leaving the quantum noise beyond the consideration. Inserting then this equation into Eq. (4) and the resulting expression into the Hamiltonian [Eq. (2)], after some algebra we arrive at

$$\hat{\mathcal{H}}_{Iv} = -\sum_k \frac{2\pi i\omega_k}{\Omega}\int_{-\infty}^{t}\int_V\int_V \hat{\mathcal{P}}_\alpha(\mathbf{r},t)\hat{\mathcal{P}}_\beta(\mathbf{r}',\tau) \times \sum_\lambda e_{k\lambda}^{(\alpha)}e_{k\lambda}^{(\beta)}e^{i\mathbf{k}(\mathbf{r}-\mathbf{r}')}e^{i\omega_k(\tau-t)}d\tau d^3\mathbf{r}d^3\mathbf{r}' + \text{H.c.}, \tag{7}$$

where indices α and β mark Cartesian projections of vectors. The summation over repetitive indices is assumed. Using the relationship[1]

$$\sum_\lambda e_{k\lambda}^{(\alpha)}e_{k\lambda}^{(\beta)} = \delta_{\alpha\beta} - \frac{k_\alpha k_\beta}{k^2} = \frac{1}{k^2}\left(\frac{\partial^2}{\partial x_\alpha \partial x_\beta} - \delta_{\alpha\beta}\frac{1}{c^2}\frac{\partial^2}{\partial t^2}\right),$$

we proceed to the limit $\Omega \to \infty$ in Eq. (7). That corresponds to the replacement

$$\sum_k [\cdot] \to \frac{\Omega}{(2\pi)^3}\int [\cdot]d^3\mathbf{k}.$$

Then, utilizing the Markov property of the polarization operator, $\hat{\mathcal{P}}_\alpha(\mathbf{r},t) \simeq \hat{\mathcal{P}}_\alpha(\mathbf{r},0)$ [14], the Hamiltonian [Eq. (7)] is reduced to

$$\hat{\mathcal{H}}_{Iv} = -4\pi\int_0^\infty\int_V\int_V \left(\frac{\partial^2}{\partial x_\alpha \partial x_\beta} - \delta_{\alpha\beta}\frac{1}{c^2}\frac{\partial^2}{\partial t'^2}\right) \times G^{(0)}(\mathbf{r}-\mathbf{r}',t')\hat{\mathcal{P}}_\alpha(\mathbf{r},t)\hat{\mathcal{P}}_\beta(\mathbf{r}',t)dt'd^3\mathbf{r}d^3\mathbf{r}', \tag{8}$$

where

$$G^{(0)}(\mathbf{r},t) = \frac{ic^2}{2(2\pi)^3}\int \frac{e^{i\mathbf{kr}}}{\omega_k}(e^{-i\omega_k t} - e^{i\omega_k t})d^3\mathbf{k} = \frac{1}{4\pi|\mathbf{r}|}\left[\delta\left(\frac{|\mathbf{r}|}{c} - t\right) - \delta\left(\frac{|\mathbf{r}|}{c} + t\right)\right], \tag{9}$$

is the free-space Green's function[38] and $\delta(\cdots)$ is the Dirac delta function. An evaluation of $\hat{\mathcal{H}}_{\text{vac}}$ in Eq. (3) is carried out analogously and gives $\hat{\mathcal{H}}_{\text{vac}} = -\hat{\mathcal{H}}_{Iv}/2$.

As a next step, we adopt the quasistatic approximation, which utilizes the property of the QD to be electrically small. The approximation implies the limit (transition) $c \to \infty$ and neglects the terms $\sim \partial^2/\partial t'^2$ in the Hamiltonian [Eq. (8)]. Then, the Hamiltonians $\hat{\mathcal{H}}_{\text{vac}}$ and $\hat{\mathcal{H}}_{Iv}$ are represented by the sum as follows:

$$\Delta\hat{\mathcal{H}} = \hat{\mathcal{H}}_{\text{vac}} + \hat{\mathcal{H}}_{Iv} = -\frac{1}{2}\int_V\int_V \hat{\boldsymbol{\mathcal{P}}}(\mathbf{r})\underline{G}(\mathbf{r}-\mathbf{r}')\hat{\boldsymbol{\mathcal{P}}}(\mathbf{r}')d^3\mathbf{r}d^3\mathbf{r}', \tag{10}$$

where

$$\underline{G}(\mathbf{r}-\mathbf{r}') = \nabla_\mathbf{r}\otimes\nabla_\mathbf{r}\left(\frac{1}{|\mathbf{r}-\mathbf{r}'|}\right) \tag{11}$$

is the free space Green's tensor; $\nabla_\mathbf{r}\otimes\nabla_\mathbf{r}$ is the operator dyadic acting on the variable $\mathbf{r}$. In the quasistatic approximation, we neglect the line broadening due to dephasing and spontaneous emission. The latter effect can be introduced in the model by retaining terms $O(1/c)$ in the the quasistatic approximation.

In the preceding analysis, we have suggested that the exchange by virtual photons of all modes occurs between all allowed dipole transitions. That is, on that stage, the problem was stated as a quantum-mechanical many-body problem. The analysis can be significantly simplified if we restrict ourselves to the two-level approximation, assuming the exciton transition frequency to be resonant with the acting field carrier frequency, and utilize the self-consistent field model. The self-consistent field is introduced by means of the Hartree-Fock-Bogoliubov (HFB) approximation, which implies the linearization of the Hamiltonian [Eq. (10)] by the substitution

$$\hat{\boldsymbol{\mathcal{P}}}(\mathbf{r})\hat{\boldsymbol{\mathcal{P}}}(\mathbf{r}') \to \hat{\boldsymbol{\mathcal{P}}}(\mathbf{r})\langle\hat{\boldsymbol{\mathcal{P}}}(\mathbf{r}')\rangle + \langle\hat{\boldsymbol{\mathcal{P}}}(\mathbf{r})\rangle\hat{\boldsymbol{\mathcal{P}}}(\mathbf{r}'). \tag{12}$$

The HFB approximation (see, e.g., Ref. 39) is widely used for the description of properties of quasiparticles in condensed matter such as Bose-Einstein condensates,[40] condensed polaritons in disordered microcavities,[41] excitons in bulk semiconductors, quantum wells,[42,43] and quantum dots.[44,45] In Ref. 44, which investigates the applicability of the HFB approximation for QDs, it has been demonstrated that for a small QD at zero magnetic field and small number of electrons, the approximation gives highly accurate results. Since in our paper we consider a single electron-hole pair strongly confined in the QD at zero magnetic field, our model satisfies to conditions of the mean-field approximation applicability formulated in Ref. 44. Also, we have discussed the application of the HFB approximation to our problem in previous publications[33,35] under a phenomenological derivation of the Hamiltonian describing the local field in the QD due to depolarization.

The polarization operator of a two-level system is given by[46]

$$\hat{\boldsymbol{\mathcal{P}}}(\mathbf{r}) = |\zeta(\mathbf{r})|^2(\boldsymbol{\mu}\hat{\sigma}_+ + \boldsymbol{\mu}^*\hat{\sigma}_-), \tag{13}$$

where $\hat{\sigma}_\pm$ are the Pauli pseudospin operators and $\zeta(\mathbf{r})$ is the wave function of the electron-hole pair. In the strong confinement regime, this function is assumed to be the same both in excited and ground states.[47,48]

In the two-level approximation, the carrier motion Hamiltonian is represented as

$$\hat{\mathcal{H}}_0 = \varepsilon_e \hat{a}_e^\dagger \hat{a}_e + \varepsilon_g \hat{a}_g^\dagger \hat{a}_g, \tag{14}$$

where $\varepsilon_{g,e}$ and $\hat{a}_{g,e}^\dagger / \hat{a}_{g,e}$ are the energy eigenvalues and creation/annihilation operators of the exciton, respectively; indices e and g correspond to the excitonic excited and ground states, respectively. The acting field operator is expressed by relation (4) where substitutions $\hat{v}_{k\lambda} \to \hat{c}_q(t)$ and $\hat{v}_{k\lambda}^\dagger \to \hat{c}_q^\dagger(t)$ have been made; $\hat{c}_q^\dagger(t)/\hat{c}_q$ are the creation/annihilation operators of the incident (real) photons (the polarization index λ is included in the mode number q). Formally, relation (6) is also fulfilled for operators $\hat{c}_q(t)$ and $\hat{c}_q^\dagger(t)$, and the first term describes the evolution of real photons. However, since the exchange interaction is included into the vacuum field component, the second term in relation (6) disappears in the case of real photons. Then, the Hamiltonian $\hat{\mathcal{H}}_{\text{ph}}$ is given by relation (3) after the substitutions $\hat{v}_{k\lambda} \to \hat{c}_q(-\infty)$ and $\hat{v}_{k\lambda}^\dagger \to \hat{c}_q^\dagger(-\infty)$. For brevity, we denote $\hat{c}_q(-\infty) = \hat{c}_q$ and $\hat{c}_q^\dagger(-\infty) = \hat{c}_q^\dagger$.

Note that nonresonant transitions can be approximately accounted for through a real-valued frequency-independent background dielectric function ϵ_h. Assuming ϵ_h to be equal to the dielectric function of the surrounding medium, we put further $\epsilon_h = 1$ without loss of generality. Substitutions in final expressions $c \to c/\sqrt{\epsilon_h}$ and $\boldsymbol{\mu} \to \boldsymbol{\mu}/\sqrt{\epsilon_h}$ for the speed of light and the electron-hole pair dipole moment, respectively, will restore the case $\epsilon_h \neq 1$.

As a next step, we introduce the rotating wave approximation;[1] i.e., we neglect in Eq. (8) the terms that are responsible for the simultaneous creation/annihilation of exciton-exciton and exciton-photon pairs. Then, using expressions (2), (3), and (8)–(13), after some algebra we derive the effective two-particle Hamiltonian

$$\hat{\mathcal{H}}_{\text{eff}} = \hat{\mathcal{H}}_0 + \hat{\mathcal{H}}_{\text{ph}} + \hat{\mathcal{H}}_{I0} + \Delta\hat{\mathcal{H}}, \tag{15}$$

where

$$\hat{\mathcal{H}}_{I0} = \hbar \sum_q (g_q \hat{\sigma}_+ \hat{c}_q + g_q^* \hat{\sigma}_- \hat{c}_q^\dagger) \tag{16}$$

and

$$\Delta\hat{\mathcal{H}} = \frac{4\pi}{V} \mu(\underline{\tilde{N}}\boldsymbol{\mu})(\hat{\sigma}_- \langle \hat{\sigma}_+ \rangle + \hat{\sigma}_+ \langle \hat{\sigma}_- \rangle), \tag{17}$$

where $g_q = -i\boldsymbol{\mu}\mathbf{e}_q \sqrt{2\pi\omega_k/\hbar\Omega}\, \exp(i\mathbf{k}\mathbf{r}_c)$ is the coupling factor for photons and carriers in the QD, and $\mathbf{r}_c$ is the radius vector of the QD geometrical center. The depolarization tensor is given by

$$\underline{\tilde{N}} = -\frac{V}{4\pi} \int_V \int_V |\xi(\mathbf{r})|^2 |\xi(\mathbf{r}')|^2 \underline{G}(\mathbf{r} - \mathbf{r}') d^3\mathbf{r} d^3\mathbf{r}'. \tag{18}$$

Note that the resulting Hamiltonian [Eq. (15)] coincides with that obtained in Ref. 35 in an independent way.

B. Equations of motions

Let $|\tilde{\psi}(t)\rangle$ be a wave function of a QD interacting with quantum light. In the interaction representation, the system is described by the Schrödinger equation

$$i\hbar \frac{\partial |\psi\rangle}{\partial t} = \hat{\mathcal{H}}_{\text{int}} |\psi\rangle, \tag{19}$$

with $|\psi(t)\rangle = \exp[i(\hat{\mathcal{H}}_0 + \hat{\mathcal{H}}_{\text{ph}})t/\hbar]|\tilde{\psi}(t)\rangle$ and $\hat{\mathcal{H}}_{\text{int}} = \exp[i(\hat{\mathcal{H}}_0 + \hat{\mathcal{H}}_{\text{ph}})t/\hbar](\hat{\mathcal{H}}_{I0} + \Delta\hat{\mathcal{H}})\exp[-(i\hat{\mathcal{H}}_0 + \hat{\mathcal{H}}_{\text{ph}})t/\hbar]$. We represent the wave function $|\psi(t)\rangle$ by the sum as follows:

$$|\psi(t)\rangle = \sum_{\{n_k\} \geqslant 0} [A_{\{n_k\}}(t)|e\rangle + B_{\{n_k\}}(t)|g\rangle]|\{n_k\}\rangle, \tag{20}$$

where $A_{\{n_k\}}(t)$ and $B_{\{n_k\}}(t)$ are coefficients to be found; $|\{n_k\}\rangle$ denotes the multimode field state with n photons in k mode; $|\{0_k\}\rangle$ is the wave function of the vacuum state of the electromagnetic field; and $|e\rangle$ and $|g\rangle$ are the wave functions of the QD ground and excited states, respectively. By inserting relation (20) into the Schrödinger equation [Eq. (19)], after some manipulations we arrive at the system of equations of motion,

$$\begin{aligned} i\frac{dA_{\{m_l\}}}{dt} &= \Delta\omega B_{\{m_l\}} \sum_{\{n_q\}} A_{\{n_q\}} B_{\{n_q\}}^* \\ &\quad + \sum_q g_q \sqrt{m_q + 1} B_{\{m_l + \delta_{lq}\}} e^{i(\omega_0 - \omega_q)t}, \end{aligned}$$

$$i\frac{dB_{\{m_l\}}}{dt} = \Delta\omega A_{\{m_l\}} \sum_{\{n_q\}} A_{\{n_q\}}^* B_{\{n_q\}} + \sum_q g_q^* \sqrt{m_q} A_{\{m_l - \delta_{lq}\}} e^{-i(\omega_0 - \omega_q)t}, \tag{21}$$

with

$$\Delta\omega = \frac{4\pi}{\hbar V} \boldsymbol{\mu}(\underline{\tilde{N}}\boldsymbol{\mu}), \tag{22}$$

as the local field induced depolarization shift.[28,35] Here, $\omega_0 = (\varepsilon_e - \varepsilon_g)/\hbar$ is the exciton transition frequency. It can easily be shown that system (21) satisfies the conservation law,

$$\frac{d}{dt} \sum_{\{n_k\}} (|A_{\{n_k\}}|^2 + |B_{\{n_k\}}|^2) = 0. \tag{23}$$

System (21) allows us to analyze the interaction between QD and electromagnetic field of an arbitrary spatial configuration and arbitrary polarization. Letting the coefficients $g_q(t)$ to be adiabatically slow-varying functions, we can apply Eq. (21) to QDs exposed to an electromagnetic pulse.

C. Single-mode approximation

Among different physical situations described by Eqs. (21), the single-mode excitation is of special interest. Indeed, such a case corresponds, for instance, to the light-QD interaction in a microcavity with a particular mode resonant with the QD exciton. Owing to the high Q factor, the strong light–QD coupling regime is feasible in microcavity provid-

ing numerous potential applications of such systems.[1,3]

For the case of a spherical QD interacting with single-mode light, only the components $|\{n_k\}\rangle = |0_1, 0_2, \ldots, n_q, \ldots, 0_k, \ldots\rangle = |n_q\rangle$, with q as the number of interacting mode, are accounted for in the wave function [Eq. (20)]. Then, omitting for brevity the mode number, system (22) is reduced to

$$i\frac{dA_n}{dt} = \Delta\omega B_n \sum_m A_m B_m^* + g\sqrt{n+1}B_{n+1}e^{i(\omega_0-\omega)t},$$

$$i\frac{dB_{n+1}}{dt} = \Delta\omega A_{n+1} \sum_m A_m^* B_m + g^*\sqrt{n+1}A_n e^{-i(\omega_0-\omega)t}. \quad (24)$$

Note that the conservation law [Eq. (23)] holds true for Eqs. (24), with the substitution $\{n_k\} \to n$. Equations (21) and (24) govern the time evolution of the QD driven by quantum light.

III. FREE MOTION

The free motion regime implies neglecting the QD–electromagnetic field interaction and thus imposes the condition $g=0$ on Eqs. (24). The wave function for noninteracting QD and electromagnetic field is factorized, thus allowing an analytical solution of Eq. (24) in the form of

$$A_n(t) = C_n A(t), \quad B_n(t) = C_n B(t),$$

where C_n are arbitrary constants satisfying the normalization condition $\Sigma_n |C_n|^2 = 1$. In that case, system (24) is reduced to the exactly integrable form

$$i\frac{dA}{dt} = \Delta\omega A|B|^2, \quad i\frac{dB}{dt} = \Delta\omega B|A|^2, \quad (25)$$

and its solution is given by

$$A(t) = a_0 e^{-i\Delta\omega|b_0|^2 t}, \quad B(t) = b_0 e^{-i\Delta\omega|a_0|^2 t}. \quad (26)$$

Here, a_0 and b_0 are arbitrary constants satisfying the condition $|a_0|^2 + |b_0|^2 = 1$. This solution describes a *correlated* motion of the electron-hole pair, which resulted from the local field induced self-polarization of the QD. Thus, in the QD, there appears a quasiparticle with the wave function

$$|\tilde{\psi}(t)\rangle = A(t)e^{-i\omega_e t}|e\rangle + B(t)e^{-i\omega_g t}|g\rangle. \quad (27)$$

It can easily be shown that state (27) satisfies the energy and probability conservation laws. The inversion, which is defined as the difference between excited-state and ground-state populations of the QD exciton, for the wave function [Eq. (27)] remains constant in time: $w = |A(t)|^2 - |B(t)|^2 \equiv |a_0|^2 - |b_0|^2$, whereas this state is generally nonstationary. The quasiparticle lifetime, which is not included in our model, can be estimated by $\tau_{sp} \sim 1/\Gamma_{sp}$, where Γ_{sp} is the QD-exciton spontaneous decay rate. For realistic QDs, $\Delta\omega \gg 1/\Gamma_{sp}$.[36] Consequently, the state $|\tilde{\psi}(t)\rangle$ can be treated as stationary within the range $1/\Delta\omega \ll t \ll 1/\Gamma_{sp}$.

The macroscopic polarization of the QD is described by

$$\langle\hat{\mathcal{P}}\rangle = \langle\psi|\hat{\mathcal{P}}|\psi\rangle = \frac{1}{V}\boldsymbol{\mu} a_0 b_0^* e^{-i(\omega_0-\delta')t} + \text{c.c.}, \quad (28)$$

where the parameter $\delta' = w\Delta\omega$ plays the role of the self-induced detuning, which depends on the state occupied by the exciton and on the depolarization shift. Thus, as follows from Eq. (28), the local field induced depolarization shift ($\Delta\omega \neq 0$) dictates the *nonisochronism* of the polarization oscillations, i.e., the dependence of the oscillation frequency on its amplitude. This mechanism also influences the Rabi oscillations in the system: the smaller δ' is the larger the Rabi oscillation amplitude is; such a behavior was observed experimentally in Ref. 25.

Since the inversion w lies within the range $-1 \leqslant w \leqslant 1$, the frequency ω_p of polarization oscillations in Eq. (28) may vary within the limits $\omega_0 - \Delta\omega \leqslant \omega_p \leqslant \omega_0 + \Delta\omega$. On the contrary, when $\Delta\omega = 0$, the polarization oscillates at fixed frequency ω_0. At first glance, it seems that the discrete level is transformed into a $2\Delta\omega$ band. However, this is not the case. Indeed, the concept of the band structure corresponds to linear systems where any arbitrary state is a superposition of eigenmodes with different frequencies. In contrast, the electron-hole correlation arises from the nonlinear motion of the particles in a self-consistent field. Consequently, in the presence of the light-QD interaction ($g \neq 0$), the exciton motion cannot be described by a simple superposition of different partial solutions such as Eq. (26), but has a significantly more complicated behavior. In particular, in the strong coupling regime, there are two oscillatory regimes with drastically different characteristics, separated by the bifurcation (see Sec. V).

IV. WEAK-FIELD APPROXIMATION

Consider a ground-state QD exposed to an arbitrary state of quantum light $\Sigma_{m_l}\beta_{\{m_l\}}|\{m_l\}\rangle$, where $\beta_{\{m_l\}}$ are arbitrary complex-valued coefficients satisfying the condition $\Sigma_{\{m_l\}}|\beta_{\{m_l\}}|^2 = 1$. Then, the initial conditions for Eqs. (21) are given by

$$A_{\{m_l\}}(0) = 0, \quad B_{\{m_l\}}(0) = \beta_{\{m_l\}}. \quad (29)$$

In the linear regime with respect to the electromagnetic field which is realized when $g_q \to 0$, we can assume that $B_{\{m_l\}}(t) \approx \beta_{\{m_l\}} = \text{const}$; i.e., the analysis is restricted to the time interval much less compared to relaxation time of the given exciton state. Then, system (22) is reduced to

$$\frac{dA_{\{m_l\}}}{dt} = -i\Delta\omega \sum_{\{n_q\}} A_{\{n_q\}}\beta_{\{m_l\}}\beta_{\{n_q\}}^* - \sum_q g_q\sqrt{m_q+1}\beta_{\{m_l+\delta_{lq}\}}e^{i(\omega_0-\omega_q)t}. \quad (30)$$

For further analysis, we rewrite Eq. (30) in a more convenient matrix notation,

$$\frac{d\mathbf{a}(t)}{dt} = -i\Delta\omega\boldsymbol{\rho}\mathbf{a}(t) - \mathbf{f}(t), \tag{31}$$

where $\mathbf{a}(t)$, $\mathbf{f}(t)=\Sigma_q \mathbf{f}_q e^{i(\omega_0-\omega_q)t}$, and $\boldsymbol{\beta}$ are the columnar matrices (vectors) and $\mathbf{a}(t)=(A_{\{m_l\}})$. Vectors $\mathbf{f}_q$ and $\boldsymbol{\beta}$ are defined analogously through the elements $f_q^{\{m_l\}}=ig_q\sqrt{m_q+1}\beta_{\{m_l+\delta_{ql}\}}$ and $\beta_{\{m_l\}}$, respectively; δ_{ql} is the Kronecker symbol. The quantity $\boldsymbol{\rho}=\boldsymbol{\beta}\boldsymbol{\beta}^\dagger$ is the density matrix of quantum light interacting with the QD. This matrix corresponds to the pure state of the electromagnetic field and satisfies the conditions $\boldsymbol{\rho}^n=\boldsymbol{\rho}$ $(n\geqslant 1)$ and $\boldsymbol{\rho}^0=\mathbf{I}$ (where $\mathbf{I}$ is the unit matrix). The integration of Eq. (31), imposed by initial conditions [Eq. (29)], allows us to find the analytical solution

$$\mathbf{a}(t) = -\int_0^t e^{-i\boldsymbol{\rho}\Delta\omega(t-t')}\mathbf{f}(t')dt'. \tag{32}$$

Using the truncated Taylor expansion[49]

$$e^{-i\boldsymbol{\rho}\Delta\omega(t-t')} = \mathbf{I} - \boldsymbol{\rho}(1-e^{-i\Delta\omega(t-t')}),$$

after some standard manipulations we obtain

$$\mathbf{a}(t) = -i\sum_q \left[(\boldsymbol{\rho}-\mathbf{I})\mathbf{f}_q \frac{1-e^{i(\omega_0-\omega_q)t}}{\omega_0-\omega_q-i0} - \boldsymbol{\rho}\mathbf{f}_q e^{-i\Delta\omega t}\frac{(1-e^{i(\omega_0-\omega_q+\Delta\omega)t})}{\omega_0-\omega_q+\Delta\omega-i0}\right]. \tag{33}$$

This expression describes the interaction between the QD and an arbitrary state of quantum field in the weak-field limit.

Now, let us calculate the QD effective scattering cross section defined by

$$\sigma(\infty) = \lim_{t\to\infty}\frac{d}{dt}|\mathbf{a}(t)|^2. \tag{34}$$

Substituting Eq. (33) into Eq. (34), after some algebra we arrive at

$$\sigma(\infty) = 2\pi\sum_{\nu=1,2}\sum_q |\mathbf{C}_{\nu q}|^2\delta(\omega_\nu-\omega_q), \tag{35}$$

where $\mathbf{C}_{1q}=(\boldsymbol{\rho}-\mathbf{I})\mathbf{f}_q$, $\mathbf{C}_{2q}=\boldsymbol{\rho}\mathbf{f}_q$, and $\omega_1=\omega_0$. The equation obtained demonstrates a fine structure of the absorption in a QD exposed to quantum light with arbitrary statistics. Instead of a single line with the exciton transition frequency $\omega_1=\omega_0$, a doublet appears, with one component shifted to the blue: $\omega_2=\omega_0+\Delta\omega$. The intensities of components are completely determined by the quantum light statistics. The same peculiarity has been revealed in Ref. 35 in a particular case of a QD exposed to the single-mode Fock qubit. Obviously, this result directly follows from Eq. (35) if we retain in this equation only terms corresponding the mode considered. The single-mode Fock qubit is a superposition of two arbitrary Fock states with fixed number of photons and is described by the wave function (the mode index q is omitted)

$$|\psi\rangle = \beta_N|N\rangle + \beta_{N+1}|N+1\rangle. \tag{36}$$

Consequently, if $N\geqslant 1$, the nonzero components of the vector $\mathbf{f}_q$ are $f^{(N-1)}=ig\sqrt{N}\beta_N$ and $f^{(N)}=ig\sqrt{N+1}\beta_{N+1}$. It can easily be found that in that case, Eq. (35) is reduced to Eq. (61) in Ref. 35. In the case $N=0$, the only nonzero component $f^{(0)}=ig\beta_1$ survives in Eq. (35), thus reducing this equation to Eq. (67) in Ref. 35. For the single Fock state, $|\psi\rangle=|N\rangle$ and we obtain $\mathbf{C}_2=0$, i.e., in agreement with Ref. 35, only the shifted spectral line is presented in the effective cross section.

For the QD exposed to coherent states, the recurrent formula $\beta_{n+1}=\sqrt{\langle n\rangle/(n+1)}\beta_n$ can easily be obtained, where $\langle n\rangle$ stands for the photon number mean value. Using this formula, the relation $\boldsymbol{\rho}\mathbf{f}=\mathbf{f}$ can be obtained, which gives $\mathbf{C}_1=0$. Thus, for this case, only the shifted line in the effective cross section is manifested. An analogous result has been reported in Ref. 35 for a QD, driven by a classical electromagnetic field. Such a coincidence can be treated as the manifestation of a well known concept: Among a variety of quantum states of light, the coherent states are the closest to the classical electromagnetic field.

V. QUANTUM LIGHT–QD STRONG COUPLING REGIME: RABI OSCILLATIONS

In the case when the coupling constant is comparable in value with the exciton decay rate, the linearization with respect to electromagnetic field utilized in the previous section is no longer admissible. The strong coupling regime can be realized by combining the QD with a high-Q microcavity, and one of its manifestation is the Rabi oscillations of the level population inversion in a two-level system exposed to an intense electromagnetic radiation. In this section, we utilize the system of Eqs. (24) for an investigation of the interaction between QD and single-mode quantum light. The incident-field statistics is exemplified by coherent states and Fock qubits. In the standard JC model, the Rabi oscillation picture is characterized by the following parameters:[1] (i) the coupling constant g, (ii) the frequency detuning $\delta=\omega_0-\omega$, (iii) the initial distribution of photonic states in quantum light, and (iv) the average photon number $\langle n\rangle$. Accounting for the local field correction supplements this set with the new parameter, the depolarization shift $\Delta\omega$. For convenience, we introduce the depolarization shift by means of the parameter[36] $\xi=\Omega_{\langle n\rangle}/\Delta\omega$, which compares the shift with the Rabi frequency $\Omega_{\langle n\rangle}=2|g|\sqrt{\langle n(0)\rangle}=\mu E_{\langle n\rangle}/\hbar$, where $E_{\langle n\rangle}$ is the acting field strength. To understand the dynamical property of the Rabi effect, we have investigated the following three physical characteristics: the QD-exciton inversion,

$$w(t) = \sum_{n=0}(|A_n(t)|^2 - |B_n(t)|^2), \tag{37}$$

the time evolution of the photonic state distribution,

$$p(n,t) = |A_n(t)|^2 + |B_n(t)|^2, \tag{38}$$

and the normally ordered normalized time-zero second-order correlation function of the driving field,

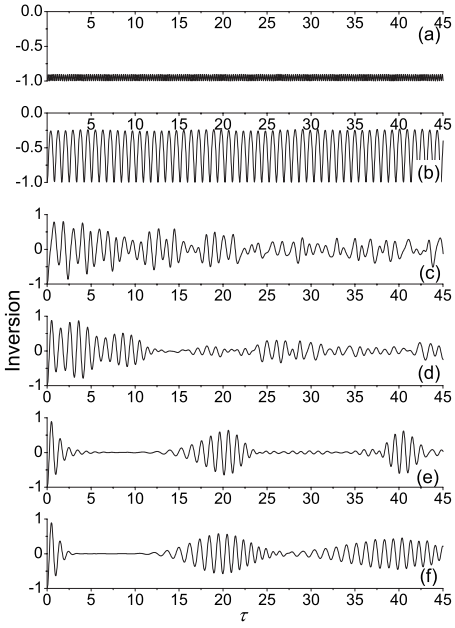

FIG. 1. Time evolution of the inversion for a QD exposed to the coherent state of light with $\langle n(0)\rangle=9$ and different values of ξ: 0.2 (a), 0.49 (b), 0.53 (c), 1.2 (d), 3.5 (e), and 40.0 (f).

$$g^{(2)}(t)=\frac{\langle \hat{c}^{\dagger}(t)\hat{c}^{\dagger}(t)\hat{c}(t)\hat{c}(t)\rangle}{\langle \hat{c}^{\dagger}(t)\hat{c}(t)\rangle^{2}}=\sum_{n=0} n(n-1)p(n,t)\Big/\left[\sum_{n=1} np(n,t)\right]^{2}. \quad (39)$$

The temporal evolution of the inversion can be detected in single QD pump-probe experiments,[21,22] while the photonic state distribution [Eq. (38)] is measurable in quantum nondemolition experiments with atoms.[50] When extracted from experiments, the characteristics [Eqs. (37)–(39)] allow estimates of the local field effect in the QD nonlinear optical response. In particular, the inversion can be detected in the single QD nonlinear spectroscopy experiments.[21,22]

A. Coherent state excitation

Let a ground-state QD be exposed to the elementary coherent state of light $\Sigma_{n=0}^{\infty}F(n)|n\rangle$, where[1] $F(n)=\exp[-\langle n(0)\rangle/2]\langle n(0)\rangle^{n/2}/\sqrt{n!}$. Then, initial conditions for Eqs. (24) are given by

$$B_n(0)=F(n), \quad A_n(0)=0. \quad (40)$$

Figures 1 and 2 show calculated inversion in a lossless QD as a function of the dimensionless time $\tau=|g|t$ at the exact synchronism ($\delta=0$) for two different initial photon mean numbers $\langle n(0)\rangle$ and for several values of parameter ξ. Our calculations demonstrate the appearance of two completely different oscillatory regimes in the Rabi effect. The first one manifests itself at $\xi<0.5$ and is characterized by periodic oscillations of the inversion within the range $-1\leqslant w(t)<0$ [see Figs. 1(a) and 1(b)]. Thus, in this regime, the inverted population is unreachable. On the contrary, in the second regime, at $\xi>0.5$, the inversion oscillates in the range $-1\leqslant w(t)\leqslant 1$ [Figs. 1(c)–1(f) and 2]. These two regimes of the Rabi effect are separated by the bifurcation, which occurs at $\xi=0.5$ for both types of incident coherent states [compare Figs. 1(b) and 1(c)].

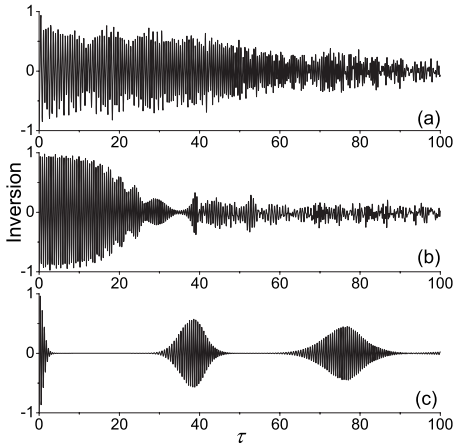

FIG. 2. Time evolution of the inversion for a QD exposed to the coherent state of light with $\langle n(0)\rangle=36$ and different values of ξ: 0.53 (a), 1.2 (b), and 40.0 (c).

In the limit $\xi\to\infty$ ($\Delta\omega\to 0$), the contribution of terms $O(\Delta\omega)$ in Eqs. (24) is small. Neglecting these terms corresponds to the elimination of the local field effect. In this case, system (24) is reduced to that follows from the standard JC model,[1] thus allowing the analytical solution,

$$w(t)=-\sum_{n=0}^{\infty}[B_{n+1}(0)]^{2}\left[\frac{\delta^{2}}{\Omega_n^{2}}+\frac{4|g|^{2}(n+1)}{\Omega_n^{2}}\cos(\Omega_n t)\right]-|B_0(0)|^{2}, \quad (41)$$

where $\Omega_n=\sqrt{\delta^{2}+4|g|^{2}(n+1)}$. The fundamental effect predicted by this solution is the collapse-revival phenomenon in the time evolution of the inversion.[1] We have found that at $\xi\geqslant 40$, the numerical simulation by Eqs. (24) leads to the same result as that of analytical simulation [Eq. (41)] [see Fig. 1(f)]. In the case $\xi\to 0$, the amplitude of Rabi oscillations tends to zero and $w(t)\approx -1$.

For a single QD imposed to classical light, the appearance of two oscillatory regimes in Rabi oscillations separated by the bifurcation at $\xi=0.5$ has been predicted in Ref. 36. According to, Ref. 36, the region $\xi>0.5$ corresponds to periodic anharmonic oscillations of the inversion. In contrast, in a QD exposed to quantum light, the collapse-revival phenomenon takes place in this region [see Figs. 1(c)–1(f) and 2]. As Figs. 1(f) and 2(c) demonstrate, the collapse and the revivals in the vicinity of the bifurcation are deformed and turn out to be drastically different from those predicted by the solution of Eq. (41).

The collapse-revival effect in the time evolution of the inversion disappears completely when $\xi<0.5$ [see Figs. 1(a) and 1(b)], where the Rabi effect picture turns out to be identical to the case of QD excited by classical light.[36]

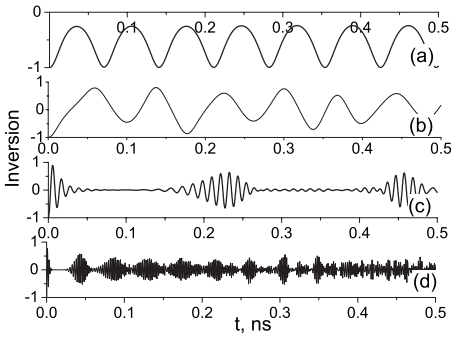

FIG. 3. Time evolution of the inversion for a spherical InGaAs QD with 6 nm radius and dipole moment $\mu \approx 12$ D, exposed to the coherent state of light with $\langle n(0)\rangle = 9$ and different values of incident-field strength $E_{\langle n\rangle}$: 0.19×10^4 V/cm (a), 0.21×10^4 V/cm (b), 1.4×10^4 V/cm (c), and 16×10^4 V/cm (d).

Let us estimate material parameters that provide observability of the effects predicted. For a spherical InGaAs QD with 6 nm radius, the dipole moment was estimated[51] to be $\mu \approx 12$ D. For this QD, we obtain $\hbar\Delta\omega \approx 0.1$ meV. Then, for the range of ξ presented in Fig. 1, from $\xi = 0.2$ to $\xi = 40$, we obtain $\hbar\Omega_{\langle n\rangle} \approx 0.02$ and $\hbar\Omega_{\langle n\rangle} \approx 4$ meV, respectively. These values are of the same order as the excitonic Rabi splitting measured in recent single QD spectroscopy experiments (see Refs. 21 and 52). On the other hand, Refs. 53 and 55–57 report the QD-exciton linewidth Γ_{hom} of the order of 1 μeV below the temperature of 10 K and lying in the range of 4–10 μeV at $T = 20$ K. Thus, the precondition to observe the strong coupling regime, $\hbar\Omega_{\langle n\rangle} \gg \Gamma_{\text{hom}}$, is fulfilled for the given range of ξ.

As an illustration, in Fig. 3, we analyze the time evolution of the inversion in a QD with material parameters given above, driven by the coherent state with $\langle n(0)\rangle = 9$, at different acting field strengths $E_{\langle n\rangle}$. Note that according to recent experimental investigations (see, e.g., Refs. 55 and 56), the typical exciton dephasing time varies from 0.1 to 1.2 ns. This result dictates the choice of the time scale in Fig. 3 and justifies the neglect of the dephasing in the system for all field strengths used in calculations. It should be emphasized that these field strengths are experimentally reachable (see, e.g., Ref. 58). As Figs. 3(a) and 3(b) demonstrate, for the given QD, the bifurcation arises in the range of the acting field strength lying between 0.19×10^4 and 0.21×10^4 V/cm (which corresponds to $\xi = 0.49$ and $\xi = 0.53$, respectively). The larger the field strength, the smaller the Rabi oscillation period [Figs. 3(c) and 3(d)]. With the driving field strength increase, the peculiarities of the Rabi oscillations resulting from the local field diminish and, at $E_{\langle n\rangle} > 16 \times 10^4$ V/cm for the given QD, the Rabi effect reduces to a conventional picture.

As seen from Fig. 3, the incorporation of the local field impact reduces the acting field strength needed for the Rabi oscillation manifestation. This conclusion agrees well with the experimental observation[25] of Rabi oscillations even in the weak excitation density regime.

An important feature of the Rabi effect in quantum light is the variation of the light statistics during the interaction with

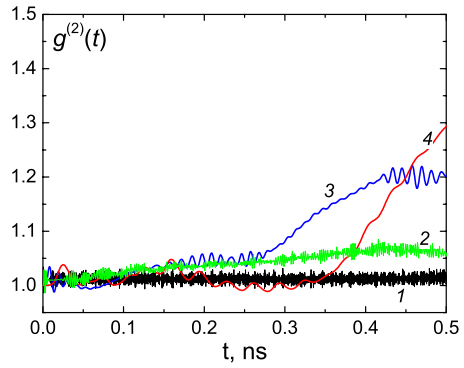

FIG. 4. (Color online) The second-order time-zero correlation function $g^{(2)}(t)$ for a spherical InGaAs QD with 6 nm radius and dipole moment $\mu \approx 12$ D exposed to the coherent state of light with $\langle n(0)\rangle = 9$ and different acting field strengths $E_{\langle n\rangle}$: 16×10^4 V/cm (1), 7.2×10^4 V/cm (2), 1.4×10^4 V/cm (3), and 0.48×10^4 V/cm (4).

a quantum oscillator, i.e., QD. We shall characterize the variation by the second-order time-zero correlation function and the photonic state distribution defined by Eqs. (39) and (38), respectively. These characteristics at different acting field strengths are depicted in Figs. 4 and 5. At relatively large incident-field strengths, $E_{\langle n\rangle} \geqslant 16 \times 10^4$ V/cm ($\xi \geqslant 40$), the behavior of the function $g^{(2)}(t)$ is identical to the case when the local field effect is eliminated from the standard JC

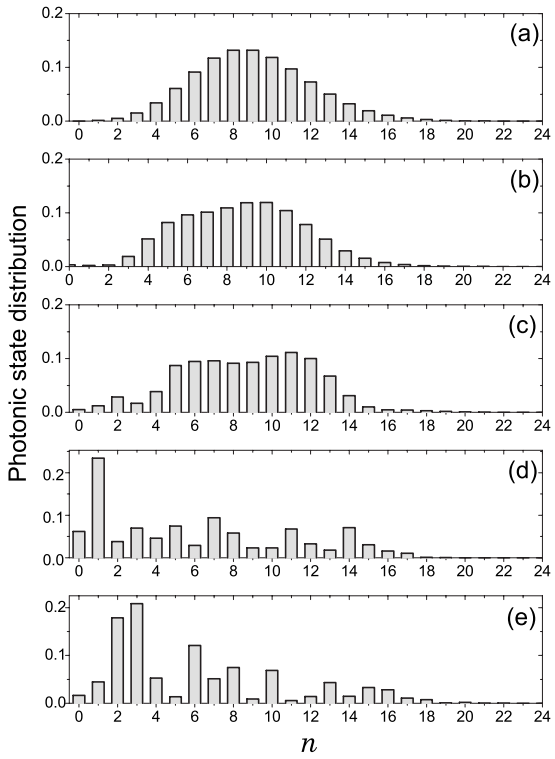

FIG. 5. Photonic state distribution for a spherical InGaAs QD with 6 nm radius and dipole moment $\mu \approx 12$ D exposed to coherent light with $\langle n(0)\rangle = 9$ for $E_{\langle n\rangle} = 0.48 \times 10^4$ V/cm ($\xi = 1.2$) and different points of time: 0 ns (a), 0.1 ns (b), 0.25 ns (c), 0.5 ns (d), and 1.0 ns (e).

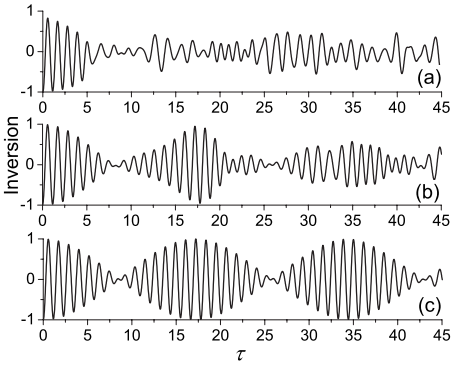

FIG. 6. Time evolution of the inversion of the QD exposed to the Fock qubit for different values of ξ: 1.2 (a), 8.0 (b), and 55.0 (c).

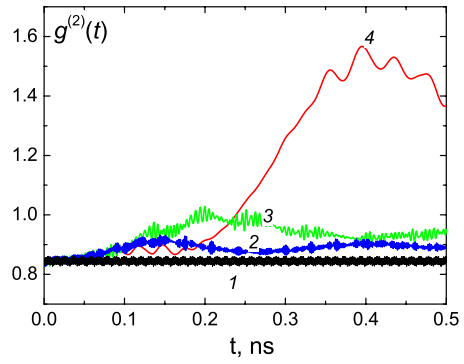

FIG. 7. (Color online) Second-order time-zero correlation function $g^{(2)}(t)$ for a spherical InGaAs QD with 6 nm radius and dipole moment $\mu \approx 12$ D, exposed to the Fock qubit for different acting field strengths $E_{\langle n\rangle}$: 22×10^4 V/cm (1), 7.2×10^4 V/cm (2), 3.2×10^4 V/cm (3), and 0.48×10^4 V/cm (4).

model[1] (see curve 1 in Fig. 4). In contrast, in the vicinity of the bifurcation, the light statistics becomes essentially super-Poissonnian [$g^{(2)}(t)>1$], as illustrated by curves 3 and 4, which correspond to $\xi=3.5$ ($E_{\langle n\rangle}=1.4\times10^4$ V/cm) and $\xi=1.2$ ($E_{\langle n\rangle}=0.48\times10^4$ V/cm), respectively. Note that curve 3 demonstrates a fast growth imposed by small-amplitude oscillations. These oscillations correspond to regions of revivals in the time evolution of the inversion [compare curve 3 in Figs. 4 and 3(c)]. At higher field strengths, $E_{\langle n\rangle}=7.2\times10^4$ V/cm, the correlation function growth is slowed down (curve 2). It should be noted that below the bifurcation threshold, when $E_{\langle n\rangle}<0.21\times10^4$ V/cm ($\xi\leqslant0.5$), the function $g^{(2)}(t)$ passes around to a unit and exhibits an oscillatory behavior.

Figure 5 presents the photonic state distribution $p(n,t)$ for different time points at a given strength of $E_{\langle n\rangle}=0.48\times10^4$ V/cm. The figure illustrates a consecutive transformation of the initially Poissonian distribution [Fig. 5(a)] into the super-Poisonnian in the course of time [see Figs. 5(c) and 5(d)]. The transformation corresponds to the increase in $g^{(2)}(t)$ illustrated by curve 3 in Fig. 4. Let us emphasize that the standard JC model predicts the photon statistics remaining Poissonian, as it takes place in our case only at large ξ (curve 1 in Fig. 4). Our calculation also shows that in the region $\xi<0.5$, the photon distribution $p(n,t)$ remains Poissonian. The invariability of the coherent light statistics in the limit $\xi\to0$ corresponds to the absence of the component $\nu=1$ in Eq. (35).

B. Quantum dot interaction with Fock qubits

Let a ground-state QD interact with electromagnetic field given by the Fock qubit [Eq. (36)]. Then, the initial conditions for Eqs. (24) are given by

$$A_n(0)=0, \quad B_n(0)=\delta_{n,N}\beta_N+\delta_{n,N+1}\beta_{N+1}. \tag{42}$$

Further, we restrict ourselves to the Fock qubit with $N=6$, assuming $\beta_N=\beta_{N+1}=\sqrt{1/2}$.

Calculations of the inversion time evolution for different values of ξ are shown in Fig. 6. At large ξ [Fig. 6(c)], the local field effect is eliminated: In agreement with the solution of Eq. (41), the inversion exhibits a harmonic modulation of the oscillation amplitude within the range $w\in[-1,1]$. The oscillation frequency is equal to $(\Omega_N+\Omega_{N+1})/2$, while the frequency of the modulation is given by $(\Omega_N-\Omega_{N+1})/2$. With parameter ξ decreasing, the modulation becomes nonharmonic, as depicted in Figs. 6(a) and 6(b).

Figures 7 and 8 illustrate change in the photonic statistics as light interacts with QD. The correlation function $g^{(2)}(t)$ is depicted in Fiq. 7 at different values of acting field strengths. Curve 1 demonstrates that, same as in Fig. 4 and in agreement with the standard JC model, the correlation function

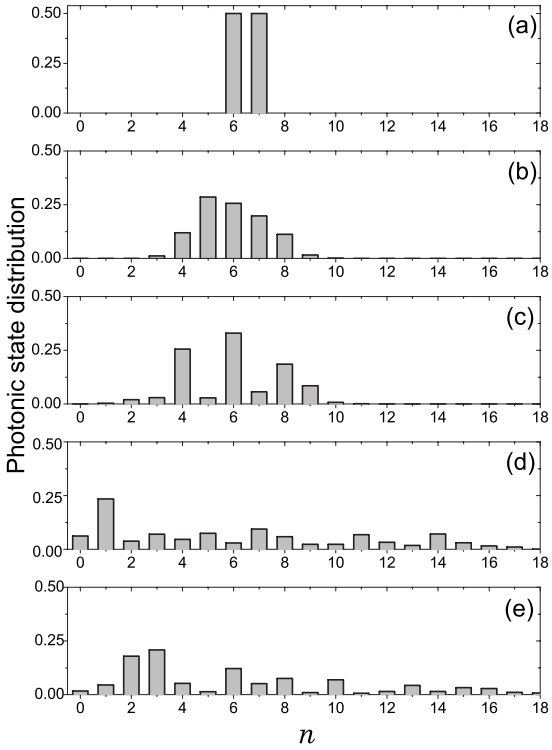

FIG. 8. Photonic state distribution for a spherical InGaAs QD with 6 nm radius and dipole moment $\mu \approx 12$ D, exposed to the Fock qubit at $E_{\langle n\rangle}=0.48\times10^4$ V/cm ($\xi=1.2$) and different points of time: 0 ns (a), 0.1 ns (b), 0.25 ns (c), 0.5 ns (d), and 1.0 ns (e).

oscillates in the vicinity of its initial value at relatively large driving field ($E_{\langle n\rangle} > 20\times 10^4$ V/cm). At relatively weak fields, the transformation of the sub-Poissonian statistics [$g^{(2)}(t) < 1$] into the super-Poissonian one [$g^{(2)}(t) > 1$], with a pronounced maximum at $t \approx 0.4$ ns, is demonstrated by curve 4. At $E_{\langle n\rangle} \simeq 7.2\times 10^4$ V/cm, curve 2 reveals two maxima, both lying in the region of sub-Poissonian statistics.

Figure 8 presents calculations of the photonic state distribution $p(n,t)$ for 0.48×10^4 V/cm (curve 4 in Fig. 7) at different points of time. The standard JC model, when describing the interaction of a Fock qubit with a two-level system, predicts variation of those probabilities $p(n,t)$ [Eq. (38)] that correspond to Fock states with $n=N$, $N\pm 1$ numbers of photons. In contrast, the incorporation of the local field effect leads to the appearance in the distribution of states $|n\rangle$ of photon numbers both smaller and larger than the present ones in the initial Fock qubit [Fig. 8(a)]. Probabilities of these states are redistributed [Figs. 8(b) and 8(c)] with time, and light statistics become irregular, which signifies the transformation of the photonic state distribution in the course of time [Figs. 8(d) and 8(e)]. In turn, this affects the Rabi oscillation picture and the second-order correlation function $g^{(2)}(t)$.

C. Vacuum Rabi oscillations

The vacuum Rabi oscillations characterize the interaction of an excited-state QD with the electromagnetic vacuum. The initial conditions for Eqs. (24) in that case are given by $B_n(0)=0$ and $A_n(0)=\delta_{n,0}$. The numerical solution of this system leads to time-harmonic oscillations of the inversion. This agrees with the analytical solution of the system at $\Delta\omega=0$, given by the standard sinusoidal law,[1]

$$w(t) = \frac{\delta^2}{\Omega_0^2} + \frac{4|g|^2}{\Omega_0^2}\cos(\Omega_0 t). \tag{43}$$

The result can be easily understood from the fact that the vacuum states, like a single Fock state, have zero observable electric field. Therefore, such states do not induce observable polarization and, consequently, frequency shift in QDs. For the same reason, zero frequency shift is inherent to single-photon states, as it has been revealed under some simplifying assumptions in Ref. 35.

VI. DISCUSSION

The standard JC model describing the interaction between a single-mode quantum electromagnetic field and a two-level system predicts the collapse-revival picture of the time evolution of the level population. The basic physical result of the analysis presented in our paper is a significant modification of the Rabi effect due to the local field induced depolarization of a QD exposed to quantum light. Two oscillatory regimes with drastically different characteristics arise. In the first regime, the time modulation of the population (the collapse and revivals) is suppressed and the QD population inversion is found negative. This indicates that trajectories of charge carriers confined by the QD occupy a finite volume in the phase space. In the second oscillatory regime, the revivals appear; however, they are found to be deformed and significantly different from that predicted by the standard JC model. The trajectories of charge carriers occupy the entire phase space. Both regimes of oscillations demonstrate the nonisochronous dependence on the coherent field strength.

Two regimes of the Rabi oscillations indicate the appearance of two types of motion of the QD exciton. The first one is a superposition of time-harmonic oscillations with the Rabi frequencies $\Omega_n = g\sqrt{N+1}$, while the second type is presented by the frequency band $|\omega_p - \omega_0| < 2\Delta\omega$. The resulting exciton motion is thus determined by a nonlinear superposition of these two types of motion.

The first mechanism of the motion is conventional for the Rabi effect; physically, it originates from the dressing of the QD exciton by the incident-field photons. This type of motion dominates at large strengths of the incident field when $\Omega_{\langle n\rangle} \gg \Delta\omega$. With the light-QD coupling constant (and, correspondingly, $\Omega_{\langle n\rangle}$) decrease, the role of the second type of motion becomes significant. This is due to electron-hole correlations resulting from the exchange interaction. It can be interpreted as the QD exciton dressing by virtual photons. This regime becomes dominating in the comparatively weak fields when $\Omega_{\langle n\rangle} \leqslant \Delta\omega$. Thus, the reduction of the threshold of the acting field strength needed for the Rabi oscillation appearance, recently observed experimentally,[25] can be attributed as a local field effect. The experiment[25] has also elucidated the nonisochronism of excitonic Rabi oscillations that can be treated as the local field effect as well [see relation (28) and numerical calculations reported in Ref. 36].

It should be noted that two oscillatory regimes in the Rabi effect may appear in other quantum systems where additional interaction mechanisms exist. As an example, consider a two-component Bose-Einstein condensate with radio-frequency coupling of two separate hyperfine states.[59] The temporal evolution of this system is governed by the coupled Gross-Pitaevskii equations, which are similar to those derived in Sec. II B. The equations combine both linear and nonlinear couplings. The linear coupling constant characterizes the interaction between the system and the electric field, while the nonlinear one accounts for the interaction between the intra- and interspecies of the condensate.[59] Depending on the ratio of the coupling parameters, the Rabi oscillations between the condensate components may exhibit both a well-ordered and a chaotic behavior,[59] similar to that depicted in Figs. 1(a) and 1(b). The formation of the Bardeen-Cooper-Schrieffer state in the fermionic alkali gases cooled below degeneracy[60] can serve as another example. In that system, the time modulation of the coupling constant leads to the Rabi oscillations of the energy gap[61] with two oscillatory regimes. The trajectories of individual Cooper pairs occupy a finite volume in the phase space in the first regime and the entire phase space in the second one.

Now, let us turn to the weak-field case. The depolarization induced local field is predicted to entail in a QD exposed to an arbitrary photonic state a fine structure of the effective scattering cross section. Instead of a single line with frequency ω_0, a duplet appears with one component shifted by a value of $\Delta\omega$. The shifted component is due to electron-hole

correlations [see Eq. (26)]. The correlations change the QD state and, consequently, provide the inelastic channel of the light scattering. The elastic scattering channel is formed by light states inducing zero observable polarization and, consequently, zero frequency shift, such as Fock states, vacuum states, etc. Now, we take into account the relation $\langle\hat{\mathbf{P}}\rangle = 4\pi\alpha\langle\hat{\mathbf{E}}_0\rangle$, which couples the observable polarization and mean value of the incident field; the quantity $\hat{\mathbf{E}}_0$ is defined through the relation $\hat{\boldsymbol{\mathcal{E}}}_0(\mathbf{t}) = \int_o^\infty \hat{\mathbf{E}}_0(\mathbf{r},\omega)d\omega + \text{H.c.}$ The scalar coefficient α is the QD polarizability of a spherical QD. Therefore, we conclude that the elastic scattering channel is formed by incident field with zero mean value (incoherent component of the electromagnetic field). Correspondingly, the coherent field component is scattered through an inelastic channel. As follows from the solution of Eq. (35), the elastic channel is not manifested for pure coherent light (the Glauber state).

Let us discuss now the local field induced alteration of the quantum light statistics. As an example, we consider the Fock qubit [Eq. (36)] as the incident-field state. For the case $\Delta\omega = 0$, the photonic state distribution is given by

$$p(n,t) = \delta_{n,N-1}|A_{N-1}(t)|^2 + \delta_{n,N}(|A_N(t)|^2 + |B_N(t)|^2) + \delta_{n,N+1}|B_{N+1}(t)|^2, \tag{44}$$

where $A_n(t)$ and $B_n(t)$ are the exact solutions of Eqs. (24) at $\Delta\omega = 0$ (see, e.g., Ref. 1). It is seen that the Fock states with photon numbers $n = N, N \pm 1$ are only presented in the distribution. The probability amplitudes of these states oscillate with the corresponding Rabi frequencies, $\Omega_{n=N,N\pm1}$. In addition to this set, extra Fock states with both smaller and larger photon numbers appear in the photonic state distribution $p(n,t)$ as the local field effect (see Fig. 8). Therefore, a bigger number of Fock states pared to those presented in the initial Fock qubit broaden the frequency spectrum of Rabi oscillations, thus providing the chaotic time evolution of the inversion.

It should be noted that the variation in the quantum light statistics occurs even in the weak-field limit $g \to 0$. To illustrate that, consider the observable polarization of the QD exciton defined in the time domain as

$$\langle\hat{\boldsymbol{\mathcal{P}}}\rangle = \frac{1}{V}\boldsymbol{\mu}^* \sum_{\{n_q\}} A_{\{n_q\}} B^*_{\{n_q\}} e^{-i\omega_0 t} + \text{c.c.} \tag{45}$$

Using Eq. (33), we couple the polarization in the frequency domain with the complex-valued amplitude of the mean incident field,

$$\langle\hat{\mathbf{P}}\rangle = \frac{|\boldsymbol{\mu}|^2/\hbar V}{\omega_0 - \omega + \Delta\omega - i0}\langle\hat{\mathbf{E}}_0\rangle. \tag{46}$$

Then, after some simple manipulations, we express the quantum fluctuations of the QD polarization by

$$\hat{\mathbf{P}} - \langle\hat{\mathbf{P}}\rangle = \frac{|\boldsymbol{\mu}|^2/\hbar V}{\omega_0 - \omega - i0}(\hat{\mathbf{E}}_0 - \langle\hat{\mathbf{E}}_0\rangle). \tag{47}$$

It follows from Eqs. (46) and (47) that the QD electromagnetic responses to the mean electric field and to its quantum fluctuation are different: The response resonant frequency is shifted by the value $\Delta\omega$ in the former case [relation (46)] and remains unshifted in the latter one, as given by relation (47). This indicates that the effective polarizability of a QD is an operator in the space of quantum states of light. It should be pointed out that this property is responsible for the alteration of the photonic state distribution in the weak-field regime and is entirely a local field effect. Note that the notions "strong (weak) coupling regime" and "strong (weak) field regime" are not identical as applied to QDs. To illustrate this statement, we express from Eqs. (46) and (47) the polarization operator in the weak-field limit,

$$\hat{\mathbf{P}} = \frac{|\boldsymbol{\mu}|^2/\hbar V}{\omega_0 - \omega - i0}\left(\hat{\mathbf{E}}_0 - \frac{\Delta\omega\langle\hat{\mathbf{E}}_0\rangle}{\omega_0 - \omega + \Delta\omega - i0}\right). \tag{48}$$

This equation is linear in the incident field but includes a term quadratic in the oscillator strength, $O(|\boldsymbol{\mu}|^4)$. Nonlinearity of that type violates the weak coupling regime. The splitting of the QD-exciton spectral line dictated by Eq. (47) is a manifestation of the strong light–matter coupling in the weak incident-field regime. Thus, the light-QD interaction is characterized by two coupling parameters, the standard Rabi frequency and a new one, the depolarization shift $\Delta\omega$.

VII. CONCLUSIONS

In this paper, we have developed a theory of the electromagnetic response of a single QD exposed to quantum light, corrected to the local field effects. The theory exploits the two-level model of QDs with both linear and nonlinear couplings of excited and ground states. The nonlinear coupling is provided by the local field influence. Based on the microscopic Hamiltonian accounting for the electron-hole exchange interaction, an effective two-body Hamiltonian has been derived and expressed in terms of the incident electric field, with a separate term responsible for the local field impact. The quantum equations of motion have been formulated and solved with this Hamiltonian for different types of the QD excitation, such as Fock qubit, coherent state, vacuum state, and arbitrary state of quantum light.

For a QD exposed to coherent light, we predict two oscillatory regimes in the Rabi oscillations separated by the bifurcation. In the first regime, the standard collapse-revival phenomenon does not reveal itself and the QD inversion is found negative. In the second regime, the collapse-revival picture is found to be strongly distorted as compared with that predicted by the standard JC model. The developed model can be easily extended to systems of other physical nature exposed to a strong electromagnetic excitation. In particular, we expect a manifestation of the local field effects in Bose-Einstein condensates[59] and fermionic alkai gases cooled below the degeneracy.[60]

We have also demonstrated that the local field correction alters the light statistics even in the weak-field limit. This is because the local fields give rise to the inelastic scattering channel for the coherent light component. As a result, coherent and incoherent light components interact with QD on different frequencies separated by the depolarization shift

$\Delta\omega$. In other words, the local fields eliminate the frequency degeneracy between these components of the incident light.

Note that our model does not account for the dephasing. According to recent experimental measurements[54,55] and theoretical estimates,[15,16] the electron-phonon interaction is the dominant mechanism of the dephasing in QDs. Thus, further development of the theory presented requires this dephasing mechanism incorporation. A next step is the generalization of our model to multilevel systems. Among them, the systems with dark excitons interacting with a weak probe pulse in the self-consistent transparency regime[17] are of special interest.

The generalization of the theory developed to the case of QD ensembles (excitonic composites), such as self-organized lattices of ordered QD molecules[62] and one-dimensional-ordered (In, Ga)As QD arrays,[63] is of special interest. One can expect that dipole-dipole interactions between QDs will manifest itself in a periodic transfer of excited state between QDs, thus resulting in the collective Rabi oscillations—Rabi waves.

All in all, we have theoretically investigated the local field effect in the electromagnetic response of a QD exposed to the quantized radiation. The developed theoretical model can serve as a basis for the analysis of luminescence and absorbtion spectra of QDs exposed to quantum states of light in both strong and weak coupling regimes. We hope that the present paper will stimulate experimental investigations of the excitonic Rabi oscillations in a QD interacting with nonclassical fields.

ACKNOWLEDGMENTS

The work was partially supported through the INTAS under Project No. 05-1000008-7801 and the Belarus Republican Foundation for Fundamental Research under Project No. F05-127. The work of S.A.M. and G.Ya.S. was partially carried out during the stay at the Institute for Solid State Physics, TU Berlin and supported by the Deutsche Forschungsgemeinschaft (DFG) in 2006 and 2007, respectively. A.M. acknowledges INTAS Grant No. 04-83-3607.

APPENDIX: DEPOLARIZATION SHIFT FOR THE SPHERICAL QUANTUM DOT

For a spherical QD, formula (22) is reduced to

$$\Delta\omega = \frac{4\pi}{3\hbar V}|\boldsymbol{\mu}|^2 \mathrm{Tr}(\tilde{\underline{N}}). \tag{A1}$$

Using expression (17), we obtain

$$\mathrm{Tr}(\tilde{\underline{N}}) = \frac{V}{4\pi}\int_V |\zeta(\mathbf{r}')|^2 \int_V |\zeta(\mathbf{r})|^2 \nabla^2 \left(\frac{1}{|\mathbf{r}-\mathbf{r}'|}\right) d^3\mathbf{r} d^3\mathbf{r}'$$

$$= V\int_V \int_V |\zeta(\mathbf{r}')|^2 |\zeta(\mathbf{r})|^2 \delta(\mathbf{r}-\mathbf{r}') d^3\mathbf{r} d^3\mathbf{r}'$$

$$= V\int_V |\zeta(\mathbf{r})|^4 d^3\mathbf{r}. \tag{A2}$$

Consider the $1s$ state. The normalized wave function in this case is given by[48]

$$\zeta(\mathbf{r}) = \frac{1}{R\sqrt{2\rho}} J_{1/2}\left(\pi\frac{\rho}{R}\right), \tag{A3}$$

where $J_\nu(\cdots)$ is the Bessel function, ρ is the spherical coordinate, and R is the QD radius. Inserting Eq. (A3) into Eq. (A2) and integrating the resulting expression, we derive the correction to the depolarization shift [Eq. (A1)],

$$\mathrm{Tr}(\tilde{\underline{N}}) = \frac{4\pi}{3}\int_0^\pi \frac{\sin^4 x}{x^2} dx \approx 2.81. \tag{A4}$$

*andrei.magyarov@gmail.com

[1] M. O. Scully and M. S. Zubairy, *Quantum Optics* (Cambridge University Press, Cambridge, 2001).
[2] D. Bimberg, M. Grundmann, and N. N. Ledentsov, *Quantum Dot Heterostructures* (Wiley, Chichester, 1999).
[3] *Single Quantum Dots, Topics of Applied Physics*, edited by P. Michler (Springer-Verlag, Berlin, 2000).
[4] M. Kasevish, Science **298**, 1363 (2002).
[5] B. Lounis and M. Orrit, Rep. Prog. Phys. **68**, 1129 (2005).
[6] S. Brattke, B. T. H. Varcoe, and H. Walther, Phys. Rev. Lett. **86**, 3534 (2001).
[7] C. K. Law and J. H. Eberly, Phys. Rev. Lett. **76**, 1055 (1996).
[8] S. Ya. Kilin, Usp. Fiz. Nauk **169**, 507 (1999) [Phys. Usp. **42**, 435 (1999)].
[9] I. V. Bagratin, B. A. Grishanin, and V. N. Zadkov, Usp. Fiz. Nauk **171**, 625 (2001) [Phys. Usp. **44**, 597 (2001)].
[10] Y. A. Wheeler and W. H. Zurek, *Quantum Theory of Measurment* (Princenton University Press, Princeton, NJ, 1983).
[11] E. T. Jaynes and F. W. Cummings, Proc. IEEE **51**, 89 (1963).
[12] Y. Yang, J. Xu, G. Li, and H. Chen, Phys. Rev. A **69**, 053406 (2004).
[13] M. Lewenstein, L. You, J. Cooper, and K. Burnett, Phys. Rev. A **50**, 2207 (1994).
[14] Weiping Zhang and D. F. Walls, Phys. Rev. A **49**, 3799 (1994).
[15] Ka-Di Zhu, Zhuo-Jie Wu, Xiao-Zhong Yuan, and Hang Zheng, Phys. Rev. B **71**, 235312 (2005).
[16] J. Förstner, C. Weber, J. Danckwerts, and A. Knorr, Phys. Rev. Lett. **91**, 127401 (2003); Phys. Status Solidi B **238**, 419 (2003).
[17] M. Fleischhauer, A. Immamoglu, and J. P. Marangos, Rev. Mod. Phys. **77**, 633 (2005).
[18] H. T. Dung, L. Knoll, and D.-G. Welsch, Phys. Rev. A **66**, 063810 (2002).
[19] Th. Unold, K. Mueller, C. Lienau, Th. Elsaesser, and A. D. Wieck, Phys. Rev. Lett. **94**, 137404 (2005).
[20] T. H. Stievater, Xiaoqin Li, D. G. Steel, D. Gammon, D. S. Katzer, D. Park, C. Piermarocchi, and L. J. Sham, Phys. Rev. Lett. **87**, 133603 (2001).
[21] H. Kamada, H. Gotoh, J. Temmyo, T. Takagahara, and H. Ando, Phys. Rev. Lett. **87**, 246401 (2001).
[22] H. Htoon, T. Takagahara, D. Kulik, O. Baklenov, A. L. Holmes,

Jr., and C. K. Shih, Phys. Rev. Lett. **88**, 087401 (2002).
[23] A. Zrenner, E. Beham, S. Stufler, F. Findels, M. Bichler, and G. Abstreiter, Nature (London) **418**, 612 (2002).
[24] X. Li, Y. Wu, D. Steel, D. Gammon, T. H. Stievater, D. S. Katzer, D. Park, C. Piermarocchi, and L. J. Sham, Science **301**, 5634 (2003).
[25] Y. Mitsumori, A. Hasegawa, M. Sasaki, H. Maruki, and F. Minami, Phys. Rev. B **71**, 233305 (2005).
[26] S. Schmitt-Rink, D. A. B. Miller, and D. S. Chemla, Phys. Rev. B **35**, 8113 (1987).
[27] B. Hanewinkel, A. Knorr, P. Thomas, and S. W. Koch, Phys. Rev. B **55**, 13715 (1997).
[28] G. Ya. Slepyan, S. A. Maksimenko, V. P. Kalosha, J. Herrmann, N. N. Ledentsov, I. L. Krestnikov, Zh. I. Alferov, and D. Bimberg, Phys. Rev. B **59**, 12275 (1999).
[29] S. A. Maksimenko, G. Ya. Slepyan, V. P. Kalosha, S. V. Maly, N. N. Ledentsov, J. Herrmann, A. Hoffmann, D. Bimberg, and Zh. I. Alferov, J. Electron. Mater. **29**, 494 (2000).
[30] H. Ajiki, T. Tsuji, K. Kawano, and K. Cho, Phys. Rev. B **66**, 245322 (2002).
[31] S. V. Goupalov, Phys. Rev. B **68**, 125311 (2003).
[32] G. Ya. Slepyan, S. A. Maksimenko, A. Hoffmann, and D. Bimberg, in *Advances in Electromagnetics of Complex Media and Metamaterials*, NATO Science Series II: Mathematics, Physics and Chemistry, Vol. 89, edited by S. Zouhdi, A. Sihvola, and M. Arsalane (Kluwer Academic, Dordrecht, 2003), pp. 385-402.
[33] S. A. Maksimenko and G. Ya. Slepyan, in *Encyclopedia of Nanoscience and Nanotechnology*, edited by J. A. Schwarz, C. Contescu, and K. Putyera (Marcel Dekker, New York, 2004), p. 3097.
[34] S. A. Maksimenko and G. Ya. Slepyan, in *The Handbook of Nanotechnology: Nanometer Structure Theory, Modeling, and Simulation*, edited by A. Lakhtakia (SPIE, Bellingham, 2004), p. 145.
[35] G. Ya. Slepyan, S. A. Maksimenko, A. Hoffmann, and D. Bimberg, Phys. Rev. A **66**, 063804 (2002).
[36] G. Ya. Slepyan, A. Magyarov, S. A. Maksimenko, A. Hoffmann, and D. Bimberg, Phys. Rev. B **70**, 045320 (2004).
[37] This approach is often utilized for the description of d-d interactions in atomic optics (see, e.g., Ref. 14).
[38] V. B. Berestetskii, E. M. Lifshitz, and L. P. Pitaevskii, *Quantum Electrodynamics* (Pergamon, Oxford, 1982).
[39] A. Griffin, Phys. Rev. B **53**, 9341 (1996).
[40] M. H. Szymanska, J. Keeling, and P. B. Littlewood, Phys. Rev. B **75**, 195331 (2007).
[41] F. M. Marchetti, J. Keeling, M. H. Szymanska, and P. B. Littlewood, Phys. Rev. Lett. **96**, 066405 (2006).
[42] B. Lummer, J.-M. Wagner, R. Heitz, A. Hoffmann, I. Broser, and R. Zimmermann, Phys. Rev. B **54**, 16727 (1996).
[43] R. Zimmermann, Phys. Status Solidi B **243**, 2358 (2006).
[44] H. F. Johnson and M. Reina, J. Phys.: Condens. Matter **4**, L623 (1992).
[45] E. Waltersson and E. Lindroth, Phys. Rev. B **76**, 045314 (2007).
[46] K. Cho, *Optical Response of Nanostructures: Microscopic Nonlocal Theory* (Springer-Verlag, Berlin, 2003).
[47] W. W. Chow and S. W. Koch, *Semiconductor-Laser Fundamentals: Physics of the Gain Materials* (Springer-Verlag, Berlin, 1999).
[48] H. Haug and S. W. Koch, *Quantum Theory of the Optical and Electronic Properties of Semiconductors* (World Scientific, Singapore, 1994).
[49] This expression is obtained (i) by the exponent expansion into Taylor series, (ii) by utilizing the relations $\boldsymbol{\rho}^n = \boldsymbol{\rho}(n \geqslant 1)$ and $\boldsymbol{\rho}^0 = \mathbf{I}$, and (iii) through subsequent summations of the Taylor series.
[50] M. Brune, S. Haroche, J. M. Raimond, L. Davidovich, and N. Zagury, Phys. Rev. A **45**, 5193 (1992).
[51] The dipole moment in the expression for the depolarization shift [Eq. (A1)] for InGaAs spherical QD can be estimated using the experimental data of [K. L. Silverman, R. P. Mirin, S. T. Cundiff, and A. G. Normann, Appl. Phys. Lett. **82**, 25 (2003)], where the value from 25 to 33 D were measured for the QDs with average lateral dimensions from 30 to 40 nm. Taking into account the theretical results concerning the dependence of the transition dipole moment on the QD surface area and shape [A. Thänharrdt, C. Ell, G. Khitrova, and H. M. Gibbs, Phys. Rev. B **65**, 035327 (2002)], we can roughly estimate the dipole moment $\mu \approx 12$ D for a spherical QD with a radius of 6 nm.
[52] T. Yoshie, A. Scherer, J. Hendrickson, G. Khitrova, H. M. Gibbs, G. Rupper, C. Ell, O. B. Shchekin, and D. G. Deppe, Nature (London) **432**, 11 (2004).
[53] D. Birkedal, K. Leosson, and J. M. Hvam, Superlattices Microstruct. **31**, 97 (2002).
[54] P. Borri, W. Langbein, S. Schneider, U. Woggon, R. L. Sellin, D. Ouyang, and D. Bimberg, Phys. Rev. B **66**, 081306(R) (2002).
[55] P. Borri, W. Langbein, U. Woggon, V. Stavarache, D. Reuter, and A. D. Wieck, Phys. Rev. B **71**, 115328 (2005).
[56] J. J. Berry, M. J. Stevens, R. P. Mirin, and K. L. Silverman, Appl. Phys. Lett. **88**, 061114 (2006).
[57] M. Bayer and A. Forchel, Phys. Rev. B **65**, 041308(R) (2002).
[58] J. Koo-Chul, J. Honglyoul, M. Treguer, T. Cardinal, and S.-H. Park, Opt. Express **14**, 7994 (2006).
[59] B. Deconinck, P. G. Kevrekidis, H. E. Nistazakis, and D. J. Frantzeskakis, Phys. Rev. A **70**, 063605 (2004).
[60] R. A. Barankov, L. S. Levitov, and B. Z. Spivak, Phys. Rev. Lett. **93**, 160401 (2004).
[61] Rabi oscillations of the energy gap correspond to the periodic creation and annihilation of the Cooper pairs.
[62] T. Mano, R. Notzel, G. J. Hamhius, T. H. Eijkemans, and J. H. Wolter, J. Appl. Phys. **95**, 109 (2004).
[63] T. V. Lippen, R. Notzel, G. J. Hamhius, and J. H. Wolter, Appl. Phys. Lett. **85**, 118 (2004).